Effect of Evaporation and Temperature-Dependent Material Properties on Weld Pool Development

T. ZACHARIA, S.A. DAVID, and J.M. VITEK

This paper evaluates the effect of weld pool evaporation and thermophysical properties on the development of the weld pool. An existing computational model was modified to include vaporization and temperature-dependent thermophysical properties. Transient, convective heat transfer during gas tungsten arc (GTA) welding with and without vaporization effects and variable properties was studied. The present analysis differs from earlier studies that assumed no vaporization and constant values for all of the physical properties throughout the range of temperature of interest. The results indicate that consideration of weld pool vaporization effects and variable physical properties produce significantly different weld model predictions. The calculated results are consistent with previously published experimental findings.

I. INTRODUCTION

UNDERSTANDING the development of the weld pool during welding is of considerable practical significance, since conduction and convection heat transfer in the weld pool can significantly influence the weld bead geometry, weld quality, and productivity.[1–4] There have been a number of attempts[5–22] to predict the effect of processing conditions on the final properties of the weldment by mathematically modeling the transport phenomena that occur during welding. As a result, considerable progress has been made in the development of computational models and algorithms for studying weld pool development during fusion joining. The earlier models of welding processes,[5–10] which involved conductive heat transfer only, are now superseded by more appropriate models in which allowance is made for convective effects, as driven by a combination of buoyancy, electromagnetic, and surface tension forces.[11–22]

Initially, most or all of the computational modeling involved the representation of two-dimensional (2-D) systems. Recently, however, three-dimensional, steady-state,[18,19] and transient[20,21,22] models have been developed for simulating the flow and heat-transfer conditions associated with welding processes. These models were applied to a variety of weld pool fluid flow and heat flow problems associated with stationary and nonstationary gas tungsten arc (GTA) welding of regular and irregular geometries. The aforementioned studies have contributed significantly to our understanding of the development of the weld pool during welding. However, the predictions of these models have to be considered as qualitative in nature, largely due to a number of idealizations involved in their development together with inadequate verification of their predictions.

Although vaporization heat flux is important during welding,[23] most studies[11,13–22] of convective heat transfer in weld pools have ignored the vaporization heat flux from the energy balance at the free surface. It has been shown[23] that weld pool evaporation results in an important cooling effect that limits the maximum temperature in the weld pool surface. To a limited extent, Thompson and Szekely[24] have incorporated the effect of vaporization by prescribing a vaporization temperature and not allowing the free surface temperature to exceed the vaporization temperature. However, this approach, in some cases, can alter the convective heat transfer in the weld pool by altering the surface tension gradient-driven flow, thereby influencing the development of the weld pool.

In computational modeling of welding, the thermophysical properties of the alloys, together with the processing parameters, are of prime importance. The effect of processing parameters on the development of the weld pool was the subject of a detailed computational study which was complemented by a systematic verification of the predictions; the results are presented in detail in Reference 25. To date, most numerical investigations have relied on constant thermophysical properties throughout the range of temperature experienced during welding. To a large extent, the assumption of constant thermophysical properties is brought about by the lack of accurate thermophysical properties, particularly at the high temperatures associated with welding. Nevertheless, it is of considerable interest to examine the extent to which the temperature-dependent physical properties of a material can influence the development of the weld pool.

The purpose of this paper is to illustrate the sensitivity of the numerical calculations to the vaporization effects and the prescribed thermophysical properties. The transient behavior of the weld pool, with and without vaporization effects and variable physical properties, was studied. A Type 304 stainless steel (SS) alloy was chosen for the present investigation, since the alloy has been the subject of a number of computational as well as experimental studies.[11,12,14–17,25] Furthermore, experimentally determined and theoretically estimated temperature-dependent thermophysical properties were readily available for Type 304 SS over the range of temperatures of interest.

T. ZACHARIA, Research Staff Member, S.A. DAVID, Group Leader, and J.M. VITEK, Research Staff Member, are with the Metals and Ceramics Division, Oak Ridge National Laboratory, Oak Ridge, TN 37831.

Manuscript submitted August 1, 1990.

II. COMPUTATIONAL MODEL

A transient, free surface computational model[20,21,22] was recently developed for investigating coupled conduction and convection heat-transfer problems associated with stationary and moving arc welding processes. The mathematical formulation considers the buoyancy, electromagnetic, and surface tension driving forces in the solution of the overall heat-transfer conditions for a specimen of finite size and shape. In the initial development of the computational model, weld pool vaporization effects and the temperature dependency of thermophysical properties were neglected. In the present analysis, the computational model[20,21,22] was appropriately modified to include temperature-dependent physical properties and evaporation of the molten metal. The essential features of the model, the governing equations and the associated boundary conditions, are presented in the next section.

A. *Modified Model*

The following assumptions were made in the present analysis:

(1) The fluid flow and heat transfer inside the molten pool are adequately described by a 2-D axisymmetric representation.
(2) The power distribution of the heat source is considered as Gaussian, based on available literature.[5-16]
(3) The surface tension is a function of temperature, with the surface-tension coefficient assumed to be a constant.

1. *Governing equations*

The definitions of all of the symbols are presented in the Appendix.

The computational model considers the densimetric coupling associated with the variation of density of the liquid metal in the formulation of all of the transportive terms of the governing equations. Therefore, the model does not resort to the conventional, simplifying, Boussinesq approximation,[26] which completely discards the thermal expansion properties of the metal. Local density, ρ, of the liquid metal is considered in terms of a constant reference value, ρ_0, and the generalized compressibility fraction, β, which represents the percentage density variation, *i.e.*,

$$\rho = \rho_0\left(1 + \frac{\Delta\rho}{\rho_0}\right) = \rho_0(1 + \beta) \qquad [1a]$$

$$\beta = \beta(T) = \frac{\Delta\rho}{\rho_0}(T) \qquad [1b]$$

The equations that describe the transient development of the weld pool due to the coupled conduction and convection heat transfer (*i.e.*, the transient temperature and flow fields in the specimen) are as follows.

Conservation of mass

$$\frac{\partial}{\partial t}\iiint_V (1 + \beta)\, dv + \iint_A (1 + \tilde{\beta})\vec{V}\cdot\hat{\mathbf{n}}\, dA = 0 \qquad [2]$$

Conservation of momentum

$$\frac{\partial}{\partial t}\iiint_V (1 + \beta)\vec{V}\, dv + \iint_A (1 + \tilde{\beta})\vec{V}\,\vec{V}\cdot\hat{\mathbf{n}}\, dA = \iint_A (p/\rho_0)(-\hat{\mathbf{n}})\cdot\hat{\mathbf{u}}\, dA + \iint_A (\sigma_n/\rho_0)\, dA + \iiint_V \vec{f}_{\text{den}}/\rho_0\, dv + \iiint_V (\vec{f}_{\text{mhd}}/\rho_0)\, dv \qquad [3]$$

where the driving force for thermally driven flow in the weld pool is given by

$$\vec{f}_{\text{den}} = \rho_0\vec{g}(1 + \beta) \qquad [3a]$$

and the electromagnetic body force is given by

$$\vec{f}_{\text{mhd}} = \vec{J} \times \vec{B} \qquad [3b]$$

Conservation of energy

$$\frac{\partial}{\partial t}\iiint_V (1 + \beta)\,[(1 - C_{\text{liq}})u_{\text{sol}} + C_{\text{liq}}u_{\text{liq}}]\, dv + \iint_A (1 + \tilde{\beta}) \cdot [(1 - C_{\text{liq}})\tilde{u}_{\text{sol}} + C_{\text{liq}}\tilde{u}_{\text{liq}}]\vec{V}\cdot\hat{\mathbf{n}}\, dA = \iint_{A_{\text{srf}}} (\vec{q}_{\text{arc}}/\rho_0)\cdot(-\hat{\mathbf{n}})\, dA + \iint_{A_{\text{srf}}} (\vec{q}_{\text{evp}}/\rho_0)\cdot(-\hat{\mathbf{n}})\, dA + \iint_{A_{\text{srf}}} (\vec{q}_{\text{srf}}/\rho_0)\cdot(-\hat{\mathbf{n}})\, dA \qquad [4]$$

2. *Boundary conditions*

The model considers the heat flux from the arc to the top surface of the metal as a specified radially symmetric Gaussian distribution given by

$$\vec{q}_{\text{arc}} = \frac{3\eta EI}{\pi r_b^2}\cdot e^{-(3(x^2+y^2)/r_b^2)} \qquad [5]$$

Previous computational modeling studies have typically used arc efficiencies, η, ranging from 70 to 95 pct. In this study, the bounding values of 70 and 95 pct were utilized for the calculations.

The evaporation heat flux is calculated based on an overall vaporization model[27] given by

$$\vec{q}_{\text{evp}} = W\Delta H_v \qquad [6]$$

where ΔH_v is the heat of evaporation. The equation given by Dushman[28]

$$\log W = A_v + \log p_{\text{atm}} - 0.5\log T \qquad [6a]$$

was used to calculate the evaporation rate. The data reported by Kim[29] for the vapor pressure for stainless steel

$$\log p_{\text{atm}} = 6.1210 - \frac{18{,}836}{T} \qquad [6b]$$

was used in the calculation. The values of H_v and A_v in Eq. [6] were estimated from the values given in Table I[28] for the major constituents in the Type 304 SS used in the study.

At the surface of the specimen, the thermal boundary conditions for the atmospheric cooling are formulated in terms of the convective heat transfer and the radiative heat transfer and are given by

$$\vec{q}_{srf} = h_c(T - T_a) + \sigma\varepsilon(T^4 - T_a^4) \qquad [7]$$

where h_c is the heat-transfer coefficient at the metal surface-atmosphere interface, T_a is the atmospheric temperature, σ is the Stefan-Boltzmann constant, and ε is the surface emittance.

Surface tension is a strong function of temperature and composition. At the surface of the weld pool, the spatial variation of surface tension must be balanced by fluid shear since the surface must be continuous. Therefore, the shear stress at the surface is equated to the gradient of surface tension.

The surface shear stress components are formulated as

$$\mu \frac{\partial V_x}{\partial z} = -\frac{\partial T}{\partial x}\frac{\partial \gamma}{\partial T} \qquad [8]$$

Along the solid-liquid interface, the conventional no-slip conditions for a viscous fluid were assumed.

The calculation domain and the grid system used are given in Figure 1. The formulation of the model directly utilizes the integral forms of the physical principles in the development of the spatially discretized computational systems of equations associated with the conventional formulations of the convective heat transfer in the weld pool. The formulation utilizes a novel discretization procedure[22] that calculates temperature and pressure in N elements (Figure 1(a)) and velocities in 2N half elements (Figure 1(b)).

3. *Stability criteria*

The computational model utilizes an explicit time-splitting numerical integration algorithm for the solutions of the governing equations.[22] The stability of the numerical scheme can be guaranteed by selecting a time step such that all stability criteria can be simultaneously satisfied. First, the selected time step must satisfy the Courant-Friedrichs-Lewy criterion for free surface flows, *i.e.*,

$$\frac{\Delta t\sqrt{g_a D_{liq,max}}}{2\min(\Delta x_{min}, \Delta y_{min}, \Delta z_{min})} \leq 1 \qquad [9]$$

Second, the selected time step must also satisfy the Courant criterion, based on maximum speed of flow $|V|_{max}$ in the melt, *i.e.*,

$$\frac{\Delta t \max[|V_{(x,y,z,)}|]}{2\min(\Delta x_{min}, \Delta y_{min}, \Delta z_{min})} \leq 1 \qquad (10)$$

and third, the selected time step must satisfy the Neumann criterion, based on maximum momentum and thermal and mass diffusivity in the melt and in the solid, *i.e.*,

$$\frac{\Delta t \max(\bar{\nu}_{max}, \bar{\kappa}_{max}, \bar{D}_{liq\text{-}sol,max})}{[2\min(\Delta x_{min}, \Delta y_{min}, \Delta z_{min})]^2} \leq 1 \qquad [11]$$

It is important to note that the maximum allowable time step cannot be accurately estimated *a priori*, since the maximum melt depth and the maximum velocities

Table I. Values for A_v and H_v

	A_v	H_v (kJ/kg)
Iron	2.52	6259.5
Nickel	2.531	6307.0
Chromium	2.505	6622.5
Manganese	2.517	4112.6

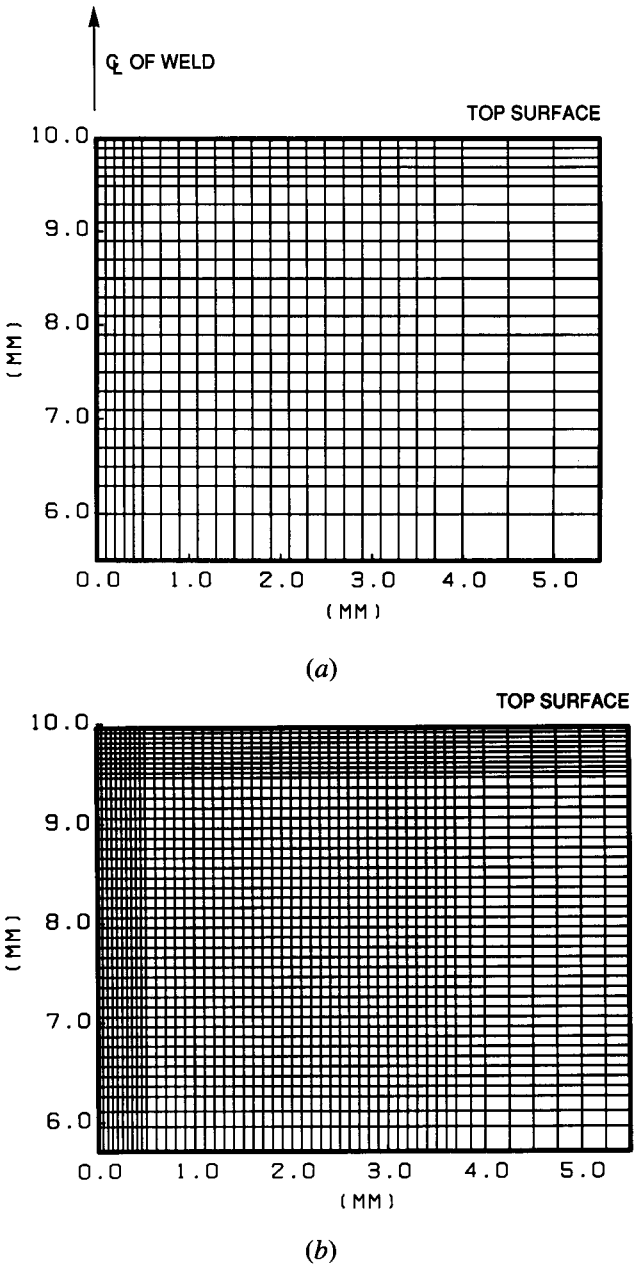

Fig. 1 — Discrete element grid system used for (*a*) calculation of temperature and (*b*) calculation of velocity components.

can change rapidly during the numerical integration. Therefore, the numerical solution requires the systematic consideration of the stability criteria at selected intervals during the numerical integration process.

III. RESULTS AND DISCUSSION

The development of the weld pool during stationary GTA welding of Type 304 SS was numerically investigated to understand the sensitivity of the predictions to weld pool vaporization and the prescribed thermophysical properties. Analyses were performed for both constant as well as temperature-dependent thermophysical properties for a weld duration of 1 second. During fusion joining, the heat source translates with respect to the base metal, resulting in relatively short arc-metal interaction times of the order of 1 to 2 seconds. Consequently, interest was focused on the initial transient development of the weld pool. The processing parameters used in the present analysis are presented in Table II.

A. *Thermophysical Properties of Type 304 Stainless Steel*

The need for a more basic understanding of welding processes by computational modeling requires the knowledge of selected thermophysical properties for the range of temperatures of interest. However, detailed information on thermophysical properties is extremely hard to obtain since there are no experimental data for the thermodynamic and transport properties for most materials at high temperatures. Consequently, most computational modeling efforts to date, attempting to study weld pool development, have used constant values for selected thermophysical properties. The question that remains to be answered is whether the temperature dependency of the physical properties have a significant influence on the development of the weld pool.

The thermophysical properties for Type 304 SS presented in Table III are from Reference 24 and are typical of the constant values used for computational modeling studies. The property data given in the table were used in this study for the purpose of comparing the predicted results for constant and temperature-dependent thermophysical properties. It must be pointed out that the value of thermal diffusivity in Table III was rounded off to the nearest decimal in Reference 24.

Table II. Welding Conditions

Welding current	150 A
Welding voltage	15.1 V
Arc efficiency	0.7 to 0.95

Table III. Physical Constants[24]

Property	Value for Steel
Density	7200 kg/m^3
Thermal diffusivity	1×10^{-5} m^2/s
Thermal conductivity	30 W/mK
Latent heat of fusion	2.47×10^5 J/kg
Viscosity	5.6×10^{-3} Ns/m^2
Specific heat	753 J/kg K

Figure 2 gives the temperature-dependent thermophysical properties between 300 and 3000 K used in the analysis.[29] Kim[29] obtained the properties of the solid state by extrapolating available experimental data, and the properties of the liquid phase were estimated based on thermodynamic principles. Even though thermodynamic data for SS's are not available in the liquid region, data are available for the constituent elements at high temperatures, and these values were used.

Surface tension is another important physical property that influences the development of the weld pool. The effect of the temperature dependency of surface tension and surface tension gradient has been a topic of active research in recent years and has led to an improved understanding of weld pool development. A detailed study of the effect of surface tension and the temperature dependency of surface tension is presented in Reference 30 and will not be repeated here. In the present study, the temperature coefficient of surface tension was treated as a constant, in order to separate its effect from that of the other selected properties (Figure 2) on the weld pool development.

B. *Evaporation of Metal during Welding*

Although it has been recognized that metal vaporizes during welding, the effect of vaporization on convective flow and heat transfer during welding has not been studied. Figure 3 shows the theoretically predicted surface temperature profiles, with and without a vaporization effect, from the center to the edge of the weld pool at time intervals of 0.25, 0.5, 0.75, and 1 second. The thermophysical properties were treated as temperature dependent, and an arc efficiency of 95 pct was used. As would be expected, the results clearly showed significant differences in the peak weld pool temperature and temperature distribution for the two cases. The results show that if the weld pool evaporation is not considered in the analysis, the weld pool quickly reaches the boiling temperature, which for stainless steel is 3080 K. On the other hand, when the vaporization effect is included in the analysis, the peak weld pool temperature is considerably lower (by as much as approximately 300 K) than the boiling temperature.

Figure 4 shows the change in peak weld pool temperature under the arc, with and without vaporization effects, as a function of weld duration. The results indicate that when weld pool evaporation is taken into account, the peak weld pool temperature increases monotonically with time until a maximum value, which is limited by the vaporization heat flux, is reached. It is interesting to note that for SS, the peak temperature under the arc does not exceed a maximum value of approximately 2850 K. This is consistent with the work of Block-Bolten and Eagar,[23] who showed that, for steels, the heat loss due to metal vaporization places an upper limit on the temperature of arc weld pools. They estimated the maximum temperature to be approximately 2780 K. Recent, experimental work[31] on measuring the weld pool surface temperatures has shown that the maximum temperature

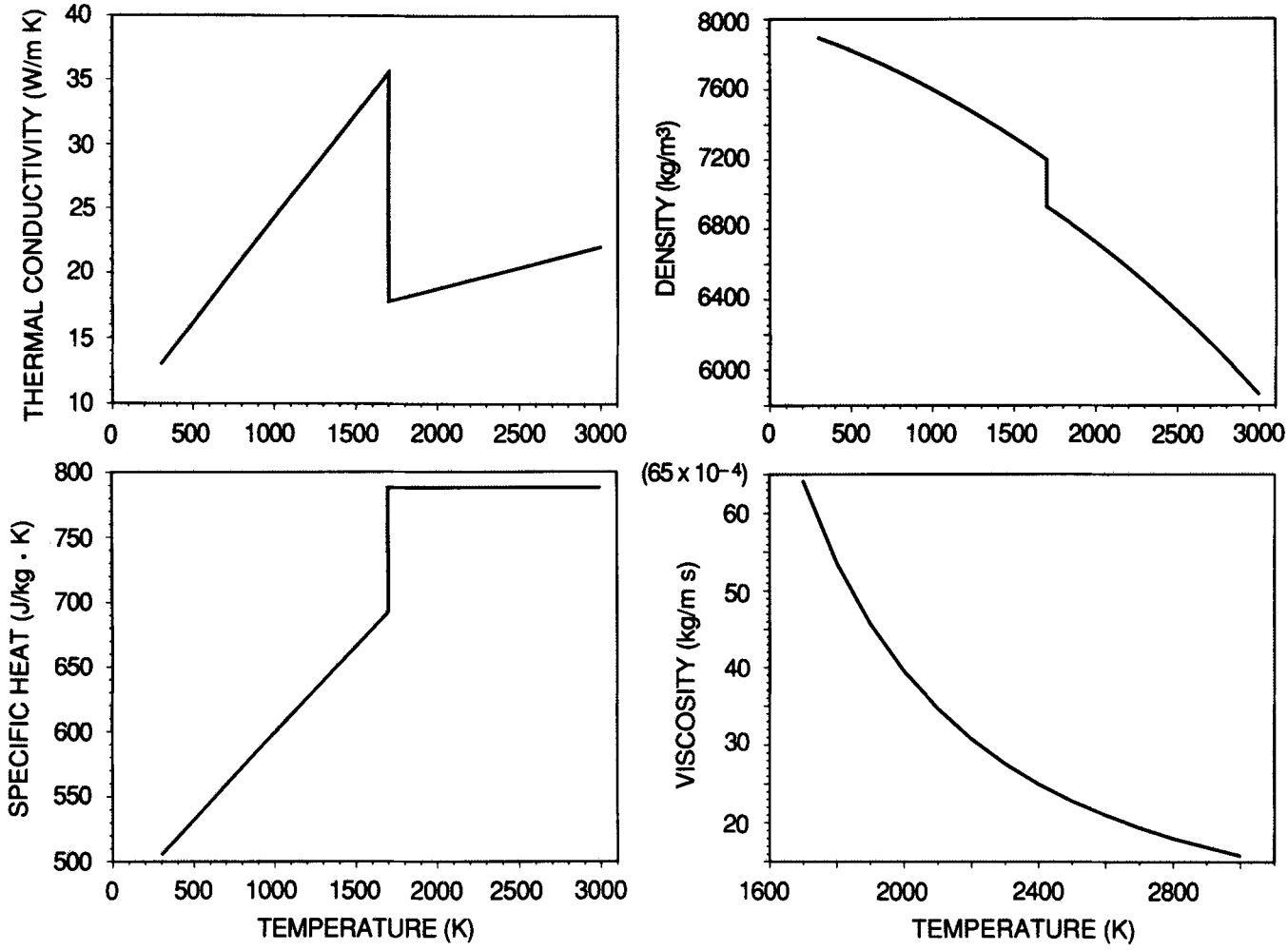

Fig. 2—Thermophysical properties of Type 304 SS.

during stationary GTA welding is closer to 2850 K. On the other hand, the results indicate that in the absence of vaporization, the peak weld pool quickly reaches the boiling temperature.

Comparison of weld penetration depth and width, with and without vaporization effects, is presented in Figure 5 as a function of weld duration. For the cases considered, the results indicate significant differences in the predicted dimensions of the weld pool. For example, after 1 second of welding, the predicted width without evaporation was higher by 26 pct and the predicted depth was higher by 30 pct when compared with the results obtained after taking evaporation into account.

The results clearly show that weld pool vaporization results in an important cooling effect and must be considered during computational modeling of weld pool fluid flow and heat flow. If the evaporation heat flux is not considered, the net heat flux into the weld pool will be higher, which can obviously change the development of the weld pool and its properties. In addition, the predicted weld pool surface temperatures would be considerably different, as seen from Figure 3, which can certainly alter the surface tension gradient-driven flow in the weld pool. Referring to Eq. [8], the surface shear stress due to the spatial variation of surface tension is formulated as a product of the spatial variation of temperature, $\partial T/\partial x$, and the temperature coefficient of surface tension, $d\gamma/dT$. If weld pool evaporation is not considered in the analysis, the spatial variation of temperature under the arc is zero (Figure 3), and consequently, based on Eq. [8], the surface shear stress becomes zero. Therefore, it is vital that computational modeling studies of weld pool development consider the effect of vaporization.

C. *Temperature Dependency of Properties and Its Influence on Weld Pool Development*

Since material properties are temperature dependent, the actual temperature experienced by the weld can influence weld pool development by altering the physical properties. This was clearly demonstrated in the previous study of surface tension effects,[30] where the development of the weld pool was found to be very sensitive to the peak surface temperatures experienced by the molten weld pool. Therefore, in the following analysis, the effect of weld pool evaporation was included.

Figure 6 shows the theoretically predicted surface temperature profiles from the center to the edge of the weld pool for constant *vs* temperature-dependent physical properties for an arc efficiency of 70 pct. The shapes

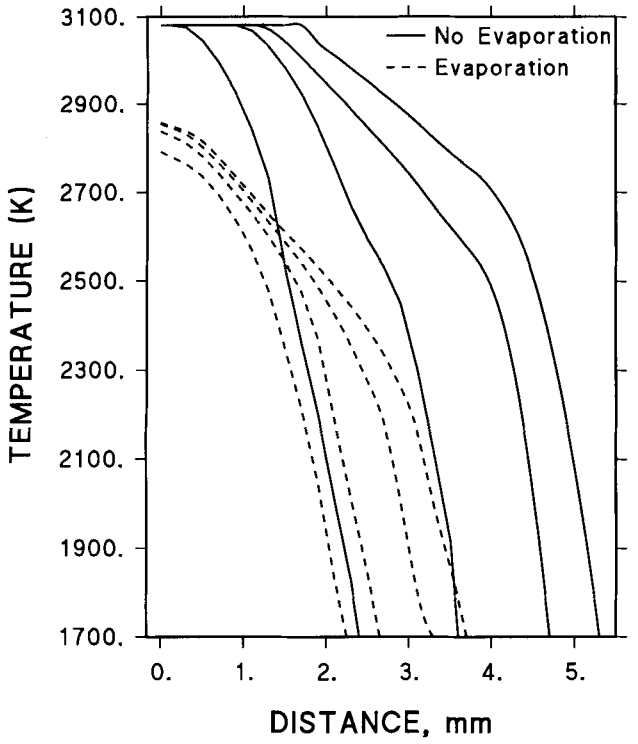

Fig. 3—Comparison of surface temperature profiles with and without vaporization effects from the center to the edge of the weld pool (η = 95 pct).

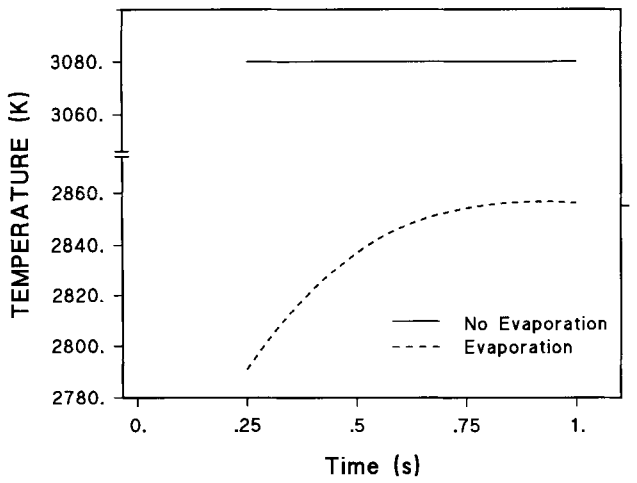

Fig. 4—Change in peak surface temperature with time during welding (η = 95 pct).

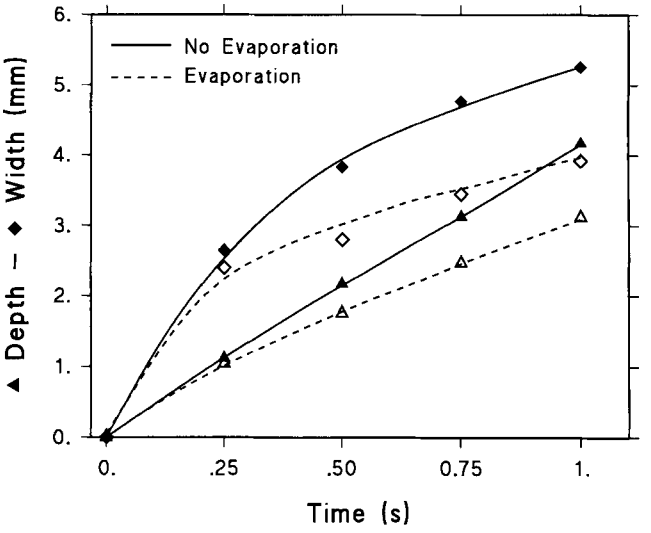

Fig. 5—Comparison of weld penetration width and depth with and without vaporization effects (η = 95 pct).

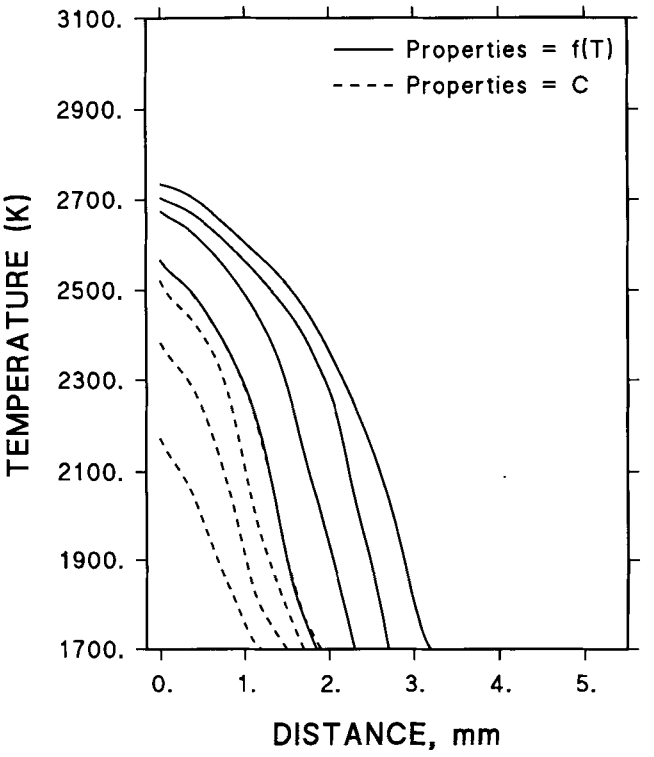

Fig. 6—Comparison of surface temperature profiles with and without temperature-dependent thermophysical properties from the center to the edge of the weld pool (η = 70 pct).

of the temperature profiles are very similar and follow a Gaussian distribution, which is to be expected, since the heat flux from the arc is assumed to be Gaussian. However, the two sets of profiles show significant differences in the maximum peak temperatures. The peak temperature obtained using constant physical properties was lower by as much as approximately 400 K. Such large differences in peak temperature, though surprising, can be easily explained based on the thermophysical properties presented in Figure 2. The material property data in Figure 2 indicate that the thermal diffusivity decreases with decreasing temperature from the melting point. Physically, this implies that with increasing distance from the fusion line (lower temperatures), the efficiency with which heat is transported decreases. Consequently, locations near the fusion line (heat-affected zone) get hotter, which can result in increased melting efficiency and increased weld pool size. On the other hand, for constant material properties, the higher thermal diffusivity transports heat away from the weld pool and its immediate vicinity very efficiently. The resulting

energy balance at the fusion line produces smaller weld pools.

Figure 7 shows the penetration depth and width as a function of temperature. For the cases considered, the results indicate significant differences in the predicted dimensions of the weld pool. For example, after 1 second of welding, the predicted depth and width for constant physical properties were 40 and 42 pct lower than that for variable properties.

Figure 8 shows the change in peak temperature as a function of time. The results show that, for variable properties, the peak temperature quickly reaches a quasi-steady state due to the local energy balance between arc heating and vaporization and other heat losses. Increasing the weld duration changes the peak temperature only very gradually, which is to be expected, since vaporization limits the peak weld pool surface temperature to approximately 2850 K for stainless steel. Since the heat removal rate from the weld pool fusion line is higher for the constant physical properties (Table III), the rise in peak weld pool temperature is more gradual annd continues to increase long after a quasi-steady state is achieved using variable properties. The results clearly show that the development of the weld pool is indeed sensitive to the temperature dependency of the material properties and such a dependency must be included for accurate predictions. In addition, the results affirm that the peak weld pool surface temperature is also strongly influenced by the weld pool vaporization effect.

The calculations were repeated for an arc efficiency of 95 pct with similar results. Figure 9 shows the penetration depth and width as a function of temperature. After 1-second weld duration, the predicted depth and width, for constant physical properties, were 24 and 30 pct lower than that for variable properties. Consideration of the results presented in Figures 7 and 9 show that, in addition to the material properties, the predicted

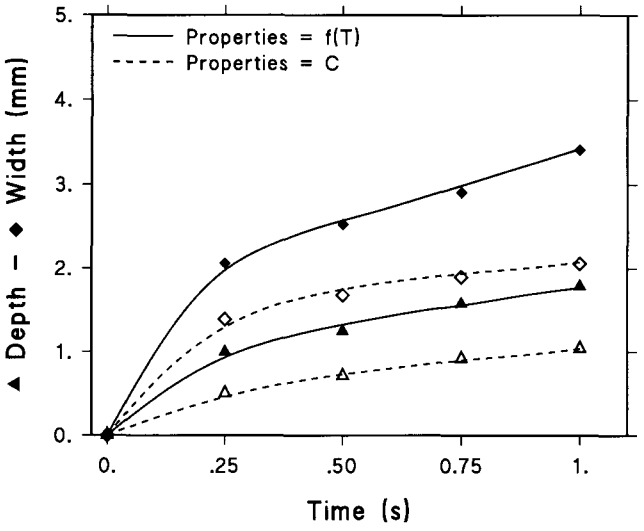

Fig. 7—Comparison of weld penetration width and depth with and without temperature-dependent thermophysical properties (η = 70 pct).

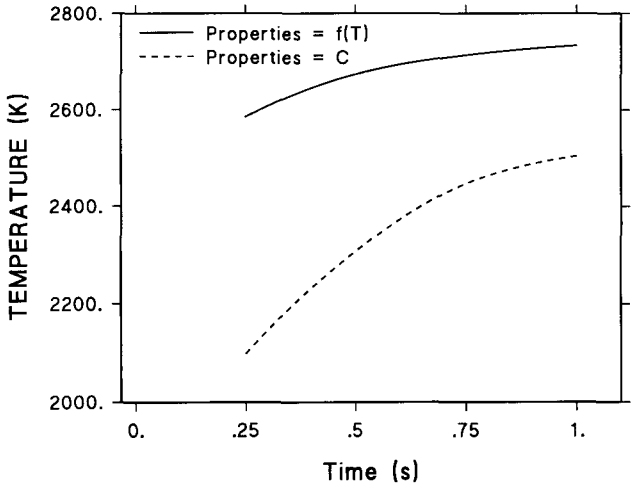

Fig. 8—Comparison of peak surface temperature as function of weld duration with and without temperature-dependent thermophysical properties (η = 70 pct).

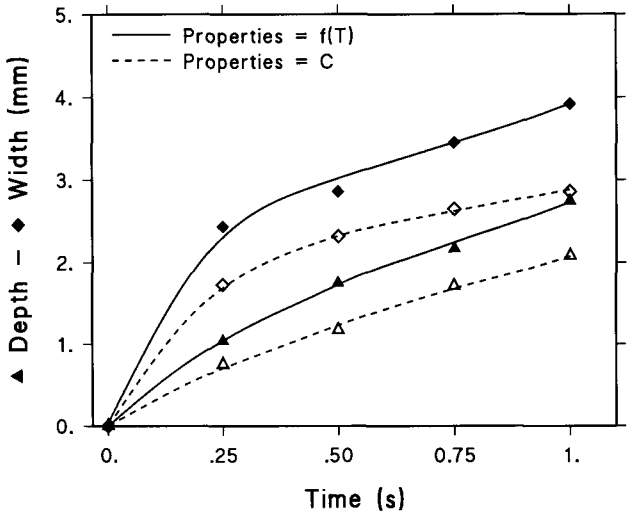

Fig. 9—Comparison of weld penetration width and depth with and without temperature-dependent thermophysical properties (η = 95 pct).

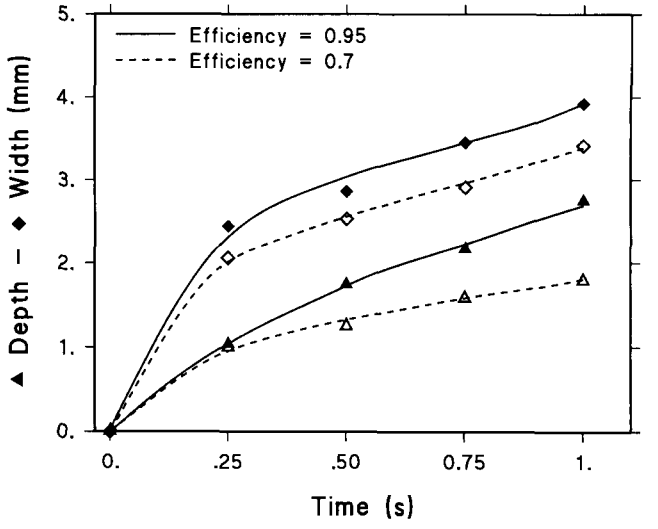

Fig. 10—Comparison of weld penetration width and depth as a function of prescribed arc efficiency.

results are also very sensitive to the prescribed arc efficiency. For temperature-dependent properties, Figure 10 shows the weld penetration depth and width as a function of weld duration, showing the influence of the prescribed arc efficiency. Therefore, it is important that the various process parameters, as well as material properties, are accurately accounted for during computational modeling of welding processes.

IV. CONCLUSIONS

A computational modeling study was conducted to analyze the convective heat transfer that occurs during welding. The emphasis of the study was to evaluate the sensitivity of the predicted results to weld pool vaporization effects and the prescribed material properties. In the context of improved understanding and ability to model the welding process with sufficient generality, it is essential that the effect of material property data on the predicted results be understood. In addition, the effect of weld pool evaporation on convective flow and heat transfer was evaluated.

The results clearly showed that weld pool evaporation can significantly influence the development of the weld pool and must be included in the numerical and physical models that describe welding. It was shown that vaporization places an upper limit on the maximum weld pool temperature, which for SS was approximately 2850 K. This is comparable to earlier experimental, as well as theoretical, predictions. If vaporization effects are not considered in the analysis, the weld pool quickly reaches the boiling temperature, which for SS is 3080 K.

The results also show that the choice of material properties can significantly influence the development of the weld pool. The analysis showed that even when seemingly accurate data are used, if the temperature dependency of the physical properties is not considered, significant discrepancy in the predictions can occur. Therefore, it is vital that computational modeling studies of the welding processes consider the temperature dependency of material properties.

APPENDIX A
NOMENCLATURE

A, A_{srf}	area
A_v	constant
B	magnetic field
c_v	specific heat
C_{liq}	liquid mass fraction
C_{sol}	solid mass fraction
D_{liq}	depth of the weld pool
E	arc voltage
f_{den}	buoyancy force
f_{mhd}	electromagnetic force
$\vec{g}$, g_a	gravitational constant
h	surface elevation
h_c	convective heat-transfer coefficient
ΔH_v	latent heat of vaporization
I	arc current
$\vec{J}$	electric current density
$\hat{\mathbf{n}}$	unit normal vector
p, p_{atm}, p_{srf}	pressure
$\vec{q}_{arc}$, $\vec{q}_{evp}$, $\vec{q}_{srf}$	heat-transfer flux
r_b	effective radius of heat flux
R	surface curvature
t	time
T	temperature
u, u_{sol}, u_{liq}	internal energy
v	volume
V	velocity
W	evaporation rate
α	thermal expansion coefficient
β	compressibility fraction
ε	surface emittance
η	arc efficiency
γ	surface tension
κ	thermal conductivity
μ	viscosity of molten metal
ν	kinematic viscosity
ρ	density
ρ_0	density at room temperature
σ	Stefan-Boltzmann constant
σ_n	shear stress
$\sim$	upwind-differencing

ACKNOWLEDGMENTS

The authors would like to thank T.G. Kollie and M.L. Santella of Oak Ridge National Laboratory for reviewing the manuscript. The research was sponsored by the Division of Materials Science, United States Department of Energy, under Contract No. DE-AC05-84OR21400 with Martin Marietta Energy Systems, Inc.

REFERENCES

1. *Trends in Welding Research in the United States*, S.A. David, ed., ASM, Metals Park, OH, 1982.
2. *Recent Trends in Welding Science and Technology*, S.A. David and J.M. Vitek, eds., ASM, Metals Park, OH, 1990.
3. *Modeling of Casting and Welding Processes*, H.D. Brody and D. Apelian, eds., TMS-AIME, Warrendale, PA, 1981.
4. *Modeling and Control of Casting and Welding Processes IV*, A.F. Giamei and G.J. Abbaschian, eds., TMS-AIME, Warrendale, PA, 1988.
5. D. Rosenthal: *Weld. J.*, 1941, vol. 20, pp. 220s-234s.
6. A.A. Wells: *Weld. J.*, 1952, vol. 31, pp. 263s-267s.
7. E. Friedman: *Weld. J.*, 1978, vol. 57, pp. 161s-166s.
8. D.R. Athey: *J. Fluid Mech.*, 1980, vol. 98, pp. 787-801.
9. S. Kou: *Metall. Trans. A*, 1981, vol. 12A, pp. 2025-30.
10. S. Kou and Y. Le: *Metall. Trans. A*, 1984, vol. 15A, pp. 1165-71.
11. G.M. Oreper and J. Szekely: *J. Fluid Mech.*, 1984, vol. 147, pp. 53-79.
12. C. Chan, J. Mazumder, and M.M. Chen: *Metall. Trans. A*, 1984, vol. 15A, pp. 2175-84.
13. S. Kou and D.K. Sun: *Metall. Trans. A*, 1985, vol. 16A, pp. 203-13.
14. R.E. Sundell, S.M. Correa, L.P. Harris, H.D. Solomon, L.A. Wojcik, W.F. Savage, D.W. Walsh, and G.-D. Lo: General Electric Report No. 86SRD013, Schenectady, NY, 1986.
15. T. Zacharia, S.A. David, J.M. Vitek, and T. DebRoy: *Metall. Trans. A*, 1989, vol. 20A, pp. 957-67.
16. A. Paul and T. DebRoy: *Metall. Trans. B*, 1988, vol. 19B, pp. 851-58.
17. S.A. Korpela, N. Ramanan, C.L. Tsai, and J.Y. Lee: Research Report, MR8810, Edison Welding Institute, Columbus, OH, May 1988.

18. S. Kou and Y.H. Wang: *Metall. Trans. A*, 1986, vol. 17A, pp. 2265-70.
19. S. Kou and Y.H. Wang: *Weld. J.*, 1986, vol. 65 (3), pp. 63s-70s.
20. T. Zacharia, A.H. Eraslan, and D.K. Aidun: *Weld. J.*, 1988, vol. 67 (1), pp. 18s-27s.
21. T. Zacharia, A.H. Eraslan, and D.K. Aidun: *Weld. J.*, 1988, vol. 67 (3), pp. 53s-62s.
22. T. Zacharia, A.H. Eraslan, D.K. Aidun, and S.A. David: *Metall. Trans. B*, 1989, vol. 20B, pp. 645-59.
23. A. Block-Bolten and T.W. Eagar: *Metall. Trans. B*, 1984, vol. 15B (9), pp. 461-69.
24. M.E. Thompson and J. Szekely: *Int. J. Heat Mass Transfer*, 1989, vol. 32 (6), pp. 1007-19.
25. T. Zacharia, S.A. David, J.M. Vitek, and H.G. Kraus: *Metall. Trans. B*, 1991, vol. 22B, pp. 243-57.
26. J.S. Turner: *Buoyancy Effects in Fluids*, Cambridge University Press, Cambridge, United Kingdom, 1973.
27. M. Choi, R. Grief, and M. Salcuden: *Numer. Heat Transfer*, 1987, vol. 11, p. 477.
28. S. Dushman: *Scientific Foundations of Vacuum Technique*, John Wiley & Sons, New York, NY, 1962.
29. C.S. Kim: *Thermophysical Properties of Stainless Steels*, Argonne National Laboratory, Argonne, IL, Report No. ANL-75-55, 1975.
30. T. Zacharia, S.A. David, J.M. Vitek, and T. DebRoy: *Weld. J.*, 1989, vol. 68 (12), pp. 499s-509s.
31. H.G. Kraus: *Weld. J.*, 1989, vol. 68 (7), pp. 269s-279s.